Chapter 5

Injector Systems

5.1 Introduction

The Next Linear Collider Injector System is designed to produce low emittance, 8-GeV electron and positron beams at 120 hertz for injection into the NLC main linacs. Each beam consists of a train of 190 bunches spaced by 1.4 ns; each bunch has a population of 0.75×10^{10} particles. The emittances at injection into the main linacs are $\gamma\varepsilon_x = 3 \times 10^{-6}$ m-rad in the horizontal and $\gamma\varepsilon_y = 2 \times 10^{-8}$ m-rad in the vertical, and the bunch length is in the range of 90-140 μm. Electron polarization of greater than 80% is required. Electron and positron beams are generated in separate accelerator complexes, each of which contains the source, damping ring systems, L-band, S-band, and X-band linacs, bunch length compressors, and collimation regions.

The need for low technical risk, reliable injector subsystems has been a major consideration in the design effort. Technologies chosen for the design of the NLC injector systems are solidly based on experience with previously built and operated high-energy colliders and with third-generation synchrotron light sources. Polarized electrons are produced using a dc photocathode gun which is very similar to the successful SLC polarized source [1]. Unpolarized positrons are generated using multiplexed target systems which will be run in parallel; the peak energy deposition in each target assembly is designed to be identical to that of the SLC positron system which ran for more than 5 years without trouble [2]. The parameters of the two main damping rings are similar to the present generation of synchrotron light sources and the B-Factory colliders in that they must store high-current beams (~ 1 A) while attaining small normalized emittances. The acceleration gradient in the injector S-band linacs [3] is only modestly higher than the gradient in the SLC linac and the S-band klystrons are based on the 65-MW SLAC 5045 [4] klystrons. Injector L-band linacs [3] have been designed with low gradients to avoid problems associated with high fields in the structures or ancillary rf distribution systems. The X-band rf for the bunch length compressors is adapted from the NLC main linac rf development.

Descriptions of the choice of injector layouts, the polarized electron source, the positron system, damping ring systems, and bunch length compression systems follow. The possibility of polarized positrons is followed by a discussion of present and future injector system activities. An explicit description of the 6-GeV injector prelinacs has not been included. While key to the functioning of the injector systems, the prelinacs are not seen to be fundamentally difficult. The designs of the prelinacs are based on proven S-band technologies for which performance is well demonstrated and understood in the operating range of the NLC injector design.

5.2 Injector Layout Choices

The present NLC configuration includes two injector-system layouts: a remote, near-surface cut-and-cover design for the California 135 site and a centralized deep-bored-tunnel design for the North-South Fermilab site. A design requirement for both is that technical components are not shared among electron and positron generation, damping, and initial acceleration systems. Cost optimization leads to separate electron and positron injector complexes. Figures 5.1a and 5.1b show the layout of the electron and positron injector complexes for the near-surface scenario. Figures 5.2a and 5.2b show the layout of the electron and positron injector complexes for the deep- bored-tunnel scenario.

In the near-surface cut-and-cover configuration, the electron and positron systems are located in separate complexes at the upstream ends of the respective main linacs, separated by about 30 km. Whereas it is reasonable to consider combining the two injector complexes at a central location, such a layout requires the addition of lengthy and costly low emittance-preserving transport lines. With no obvious cost or operational advantage for the combined complexes, it has been decided to adopt the remote and separated injectors for their low cost. As depicted in Figs. 5.1a and 5.1b, cost savings are taken wherever possible through the sharing of accelerator housings and klystron galleries among injector subsystems (e.g., in Fig. 5.1b, the e^- drive linac, e^+ targets and e^+ booster linac share a common accelerator tunnel and equipment support housing with the e^+ prelinac; in Fig. 5.1a, the e^- booster and e^- prelinac share a common accelerator tunnel and support housing).

The layout for the deep-bored-tunnel design is quite similar, except that the separate electron and positron injector complexes are placed closer to the center for the purpose of placing them on the Fermilab site and utilizing its existing facilities. The two injectors are separated by about 5 km and have separate housings for each beam line. Each injector has approximately 20 km of low-emittance-preserving transport lines and turnout beam lines at their ends for the purpose of connecting into the 180° bunch compressor arcs at the entrances to the main linacs.

A fully centralized injector is under consideration for the Fermilab site. This compact layout is located on or near the surface. Beam lines are required to drop the damped injector beams down to the long-haul transport lines placed in the main linac tunnel. The accelerator components for both electron and positron injectors are located in a common housing with shared equipment galleries and facility infrastructure.

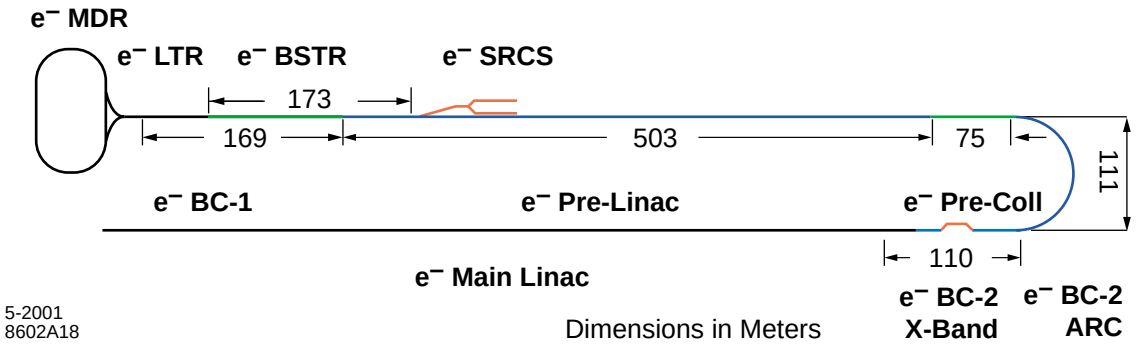

Figure 5.1a: Electron injector complex layout for the near surface cut-and-cover design. e^- SRCS is a pair of electron sources; e^- BSTR is the 2-GeV, S-band booster linac; e^- LTR is the linac-to-ring transport line; e^- MDR is the electron main damping ring; e^- BC-1 is the first stage bunch length compressor; e^- PreLinac is the 6-GeV S-band prelinac; e^- Pre-Coll is the e^- precollimation region; e^- BC-2 Arc is the second stage bunch length compressor arc; and e^- BC-2 X-band denotes the second compressor stage X-band rf section and magnet chicane.

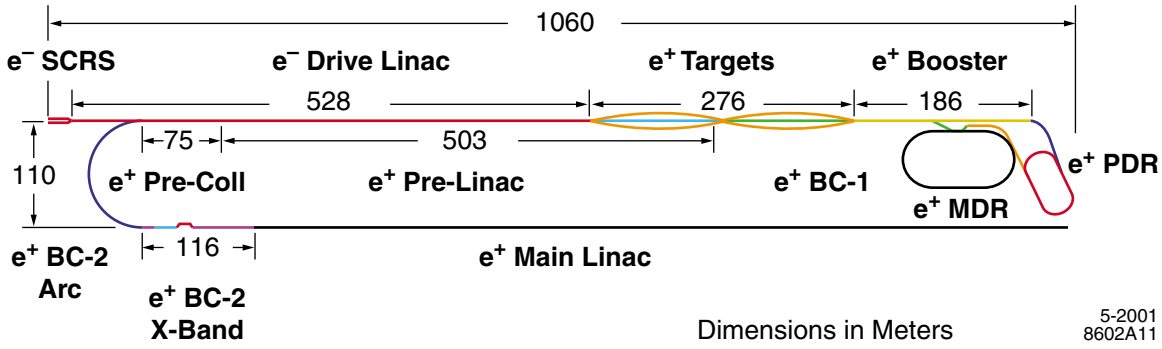

Figure 5.1b: Positron injector complex layout for the near-surface, cut-and-cover design. e^-SRCS is a pair of nonpolarized electron sources; e^-Drive Linac is a 6-GeV, S-band linac; the e^+ Targets region contains 4 identical target/capture stations of which 3 are required for normal NLC e^+ operations; e^+ BSTR is the 2-GeV, L-band booster linac; e^+ PDR is the positron predamping ring; e^+ MDR is the positron main damping ring; e^+ BC-1 is the first stage bunch length compressor; e^+ PreLinac is the 6-GeV S-band prelinac; e^+ Pre-Coll is the e^+ precollimation region; e^+ BC-2 Arc is the second stage bunch length compressor arc; and e^+ BC-2 X-band denotes the second compressor stage X-band rf section and magnet chicane.

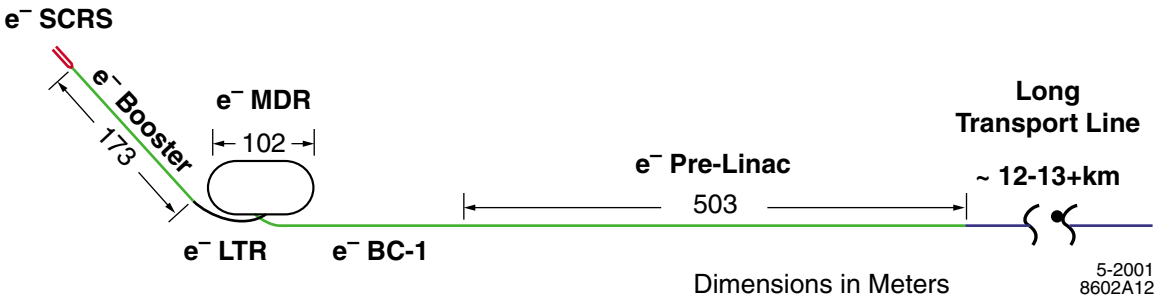

Figure 5.2a: Electron injector complex layout for the deep-bored-tunnel design. e^- SRCS is a pair of electron sources; e^- BSTR is the 2-GeV, S-band booster linac; e^- LTR is the linac-to-ring transport line; e^- MDR is the electron main damping ring; e^- BC-1 is the first stage bunch length compressor; e^-PreLinac is the 6-GeV S-band prelinac; the e^- precollimation region, the second stage bunch length compressor arc and the second compressor stage X-band rf section and magnet chicane are located at the end of the Long Transport Line and are not shown in this view.

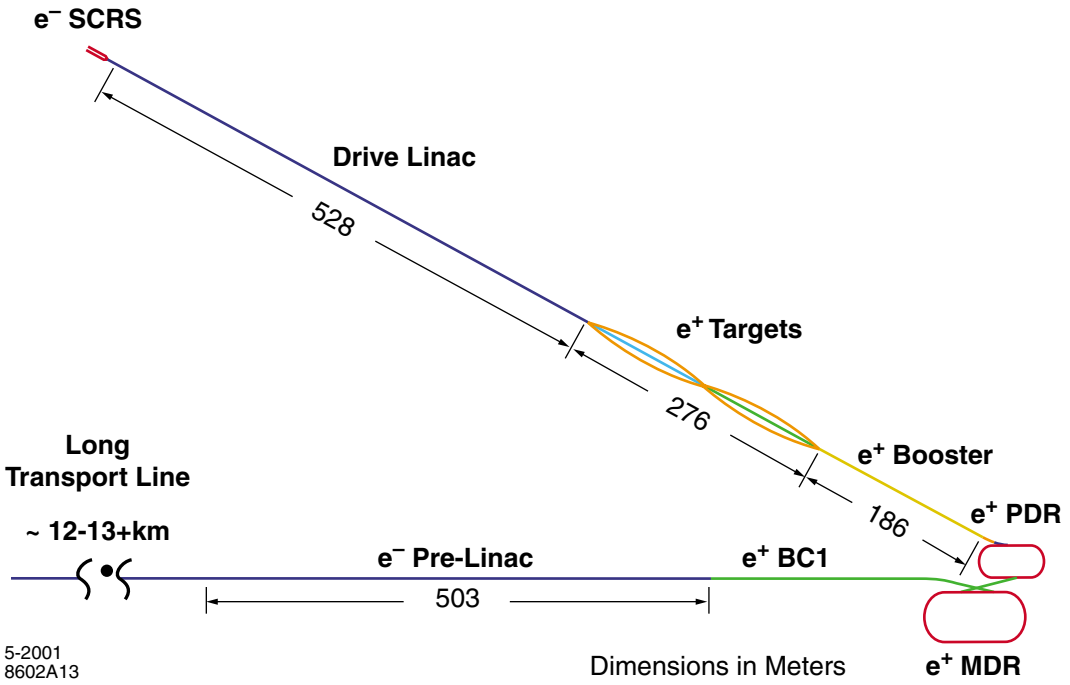

Figure 5.2b: Positron injector complex layout for deep-bored-tunnel design. e^- SRCS is a pair of nonpolarized electron sources; e^- Drive Linac is a 6-GeV, S-band linac; the e^+ Targets region contains 4 identical target/capture stations of which 3 are required for normal NLC e^+ operations; e^+ BSTR is the 2-GeV, L-band booster linac; e^+ PDR is the positron predamping ring; e^+ MDR is the positron main damping ring; e^+ BC-1 is the first stage bunch length compressor; e^+ PreLinac is the 6-GeV S-band prelinac; the e^+ precollimation region, the second stage bunch length compressor arc and the second compressor stage X-band rf section and magnet chicane are located at the end of the Long Transport Line and are not shown in this view.

5.3 Polarized Electron Source

The NLC injector electron source system creates polarized electron beams of the required energy and emittance for injection into the electron damping ring system. The polarized electron beams are produced with a photocathode electron gun, bunched in a subharmonic rf system and accelerated in an S-band linac to 1.98-GeV, the energy of the damping ring. Each beam consists of a bunch train of 190 bunches with 0.8×10^{10} particles per bunch that are spaced by 1.4 ns (or 95 bunches with 1.6×10^{10} particles per bunch that are spaced by 2.8 ns). The electrons at the end of the source booster linac have an emittance of 100×10^{-6} m-rad and spin polarization of 80%. A summary of the design parameters is given in Table 5.1.

The polarized electron source consists of a polarized high-power laser and a high-voltage dc gun with a semiconductor photocathode. Many of the performance requirements for the NLC injector are similar to those in the SLC and the design of the NLC injector is based on the successful SLC injector. The main difference is that, while the SLC polarized electron injector produced one pair of electron bunches separated by 60 ns at 120 Hz repetition rate, the NLC injector must produce 265-ns-long trains of 190 bunches separated by 1.4 ns. Individual bunch populations for the NLC are down by a factor of about 6 from the

SLC but the peak current is comparable due to the higher bunching frequency. The NLC design uses 714 MHz rf for the subharmonic bunching systems to permit the generation of beams with either 1.4 ns or 2.8 ns separation.

Table 5.1: Beam parameters as delivered by the electron source system to the electron main damping ring system for the 1.4 and 2.8 ns bunch spacing options.

PARAMETER NAME	SYMBOL	VALUE	UNITS
Bunch Spacing	T_b	1.4 (2.8)	ns
Energy	E	1.98	GeV
Energy Adjustability	ΔE	± 5	%
Bunch Energy Variation	$\delta E/E$	1	% Full Width
Single Bunch Energy Spread	$\sigma_{\Delta E/E}$	1	% Full Width
Emittance (norm. rms)	$\gamma\varepsilon_{x,y}$	100.0	10^{-6} m-rad
Bunch Length	σ_z	<10	mm
Particles/Bunch	n_B	0.8 (1.6)	10^{10} particles
Train Population Uniformity	$\Delta n_T/n_T$	1	% Full Width
Bunch-to-Bunch Pop. Uniformity	$\Delta n_B/n_B$	2	% rms
Number of Bunches	N_b	190 (95)	#
Repetition Rate	f	120	Hz
Horizontal Beam Jitter	$\Delta\gamma J_x$	50	10^{-6} m-rad
Vertical Beam Jitter	$\Delta\gamma J_y$	50	10^{-6} m-rad
Polarization	P_e	80	%
Beam Power	P_b	58	kW

The SLC polarized source generated 80% beam polarization. As long as ultra-high vacuum conditions were maintained, cathode lifetimes exceeded thousands of hours. System availability approached 99%. The basic technologies of the SLC injector will be utilized for the NLC. The most notable differences in the design are the increase in gun high voltage from the SLC value of 120 kV to 175-200 kV and the use of 714 MHz rf for subharmonic bunching. A 200 kV polarized electron gun is being developed at Nagoya University for the JLC [5]. Initial high voltage testing of this system has begun.

Improvement of the SLC photocathodes is required for NLC operation due to the higher pulse charge requirements. Efforts at SLAC [6] and at Nagoya University [7] are concentrating on developing cathodes with a highly doped surface layer to permit rapid dissipation of surface charge that builds up as beam is extracted. Recent tests [8] using a strained layer cathode with a 75 Å surface layer are extremely promising. Operating at 120 kV, up to 8×10^{11} electrons have been extracted by illuminating a 1-cm radius spot on the cathode. The polarization of the electrons was measured to be about 78% and no evidence of surface charge limit was observed. The maximum charge extracted was limited by available laser energy. Reduction of the laser spot to 0.5-cm radius still resulted in a maximum extracted charge of 8×10^{11}. Extrapolating back to 1-cm radius spots, one would expect to extract 4 times the charge, 3.2×10^{12} electrons. The NLC charge requirement is 2×10^{12} electrons in 265 ns from the cathode. While very encouraging, work continues aimed at an explicit demonstration of the full NLC charge, current and polarization.

Significant development is required for the NLC polarized source laser system. Table 5.2 lists the source laser requirements. In Table 5.2, the range in laser wavelength reflects uncertainty in the choice of specific cathode material to be used. The most challenging aspects of the source laser are the requirements

on parameter stability and the need for high availability. Both of these criteria were met for the SLC. Functional specifications for the source laser are being discussed and reviewed with the aim of assessing the technical difficulty of the laser and ultimately determining the level of resources (people, money, and time) which will be required for laser development. Although it is a difficult problem, it is not thought to be impossible.

Table 5.2: Polarized electron source laser system parameters

PARAMETER NAME	SYMBOL	VALUE	UNITS
Bunch Spacing	T_b	1.4 (2.8)	ns
Wavelength	λ	740 - 850	nm
Bandwidth	$\delta\lambda$	3	nm
Bunch Length	Δt	0.5	ns
Energy/Bunch	E_b	4.2 (8.4)	μJ
Energy. Uniformity	$\Delta n_B/n_B$	<0.5	%
Energy Uniformity along train		2	%
Number of Bunches	N_b	190 (95)	#
Repetition Rate	f	120	Hz
Polarization	P_γ	99.9	%

An S-band linac is used to accelerate the captured electrons up to the damping ring energy of 1.98-GeV. The loaded gradient of the linac is 17-MeV/m. This linac will use KEK-style SLED systems for rf pulse compression [9] that have been designed and operated at higher field levels than the original SLAC SLED systems. Beam emittance growth through the booster linac is not a problem due to the low charge per bunch (in comparison with SLC operation) and because of the relatively large damping-ring design acceptance. Standard quadrupole focusing elements are employed along with discrete steering dipoles along the length of the booster linac. Multibunch beam loading in the linac is compensated using the ΔT method in which the beam is injected into the accelerator before the rf has fully filled the structures. Fine tuning of the amplitude of the rf in a prescribed fashion after the beam has been injected provides additional control over the energy spread. An energy compression system has been included in the transport line that leads from the end of the linac to the main damping ring to further stabilize the energy and energy spread of injected bunches.

To preserve electron helicity, the spin must be rotated into the vertical direction prior to injection into the damping ring. This is accomplished using superconducting solenoids located in the transport line leading from the end of the booster linac to the entrance of the damping ring. The solenoids are based on those developed for the SLC [10]. Spin rotation is also required after extraction from the damping rings. Emittance dilution due to beam rotation through the solenoids is compensated in the optics design and is therefore not a concern [11].

Development of a polarized rf gun is being pursued at several locations around the world [12,13]. A polarized rf gun offers the promise of improved operations through the reduction in the emittance of beams injected into the e^- main damping ring and simplification of the initial bunching and capture. Such guns may generate less beam halo and subsequently reduce the radiation load at the output of the booster linac and in the damping-ring complex. It is unlikely, however, that a polarized rf gun which meets NLC performance and operational requirements will be demonstrated successfully prior to construction. Once developed, a polarized rf gun could be substituted for the SLC style source of the present design.

5.4 Positron Source

The injector positron-source system creates positron beams of the required energy and emittance for injection into the positron damping rings. Positrons are produced by colliding 6.2-GeV electrons into three separate high-Z material targets, capturing the resulting positrons, and accelerating them to the 1.98-GeV energy of the predamping-ring system. Each beam consists of a bunch train of 190 bunches with 0.9 x 10^{10} particles that are spaced by 1.4 ns (or 95 bunches with 1.8 x 10^{10} particles that are spaced by 2.8 ns). The positrons have an edge emittance of 0.03 m-rad as required by the predamping ring acceptance. Table 5.3 lists the positron beam parameters required for injection into the predamping ring system.

The design of the NLC positron system is based on the system used for the SLC [14], which demonstrated excellent reliability over many years of operation. The total number of positrons required for the NLC bunch train is almost two orders of magnitude greater than the number of positrons in the single SLC bunch. The NLC design goal is to build a target system which is expected to survive a 9-month run (120 Hz, 24 hours per day, 7 days per week, with no scheduled outages for maintenance). Targets can be replaced/repaired annually in a scheduled 3-month maintenance period.

Table 5.3: Beam parameters delivered by the positron source system to the positron predamping ring system for the 1.4 and 2.8 ns bunch spacing options.

PARAMETER NAME	SYMBOL	VALUE	UNITS
Bunch Spacing	T_b	1.4 (2.8)	ns
Energy	E	1.98	GeV
Energy Adjustability	ΔE	± 5	%
Bunch Energy Variation	$\delta E/E$	1	% Full Width
Single Bunch Energy Spread	$\sigma_{\Delta E/E}$	2	% Full Width
Emittance (norm. edge)	$\gamma\varepsilon_{x,y}$	0.03	m-rad
Bunch Length	σ_z	<10	mm
Particles/Bunch	n_B	0.9 (1.8)	10^{10} particles
Train Population Uniformity	$\Delta n_T/n_T$	1	% Full Width
Bunch-to-Bunch Pop. Uniformity	$\Delta n_B/n_B$	2	% rms
Number of Bunches	N_b	190 (95)	#
Repetition Rate	f	120	Hz
Horizontal Beam Jitter	$\Delta\gamma J_x$	0.015	m-rad
Vertical Beam Jitter	$\Delta\gamma J_y$	0.015	m-rad
Beam Power	P_b	65	kW

Positrons are produced by targeting a 6-GeV electron beam onto tungsten-rhenium (WRe) alloy to create an electromagnetic shower. The positrons produced in the shower are collected using a 5.8-tesla magnetic flux concentrator, accelerated to 250 MeV in structures encased in a 0.5-tesla solenoidal magnetic field, and then injected into an L-band linac and accelerated to 1.98-GeV. The average deposited power is handled by rotating the target and removing the excess heat through water cooling. Of critical concern for target damage is the nearly instantaneous energy deposition per unit volume.

After approximately 1,000 days of operation (~5 calendar years), the SLC positron system failed due to a combination of arcing in the initial rf capture section and increased vacuum activity in the target chamber. Upon examination it was found that a water-to-vacuum leak had occurred in one of the target cooling tubes. In addition, cracking and material ejection were found on the exit face of the target. Analysis of the damaged target was conducted at the CMR hot cell facilities at LANL [15]; thermal

hydrodynamic [16] and beam-induced radiation damage simulations [17] have been made for the SLC target operating conditions.

The peak energy deposition in the SLC target was about 35 J/g under the conditions at which the target failed. This level produces a mechanical shock in the WRe target material which is about a factor of two below the expected ultimate tensile strength of pristine material. Material hardening of a factor of about 2 from target entrance to target exit was measured along the beam path. The calculated radiation damage to the material is in excess of 3 dpa (displacements per atom). Target embrittlement and subsequent loss of material integrity are consistent with the calculated exposure level. Aged WRe is expected to fail at the SLC energy deposition level.

Because of the consistency of the observed damage with expectations from the simulations, it has been decided to limit the shock in the NLC targets to that of the SLC system. In particular, the peak energy deposition and irradiation fluences will be kept by design to less than 35 J/g and 1 dpa. Investigations into the connection between radiation damage due to electrons with that from neutron/proton exposure are continuing. It is useful to tap into the data on material property degradation due to neutron/proton damage since the database of electron-induced damage is comparatively limited. Beam tests at SLAC are underway to determine the threshold for material damage and a model of the expected damage is being developed. To date, samples of Ti, Cu, GlidCop, Ni, Ta, W, and WRe have been irradiated in the FFTB area at SLAC. Additional studies will be aimed at developing an optimized target material [18]. Induced damage to candidate target materials will be studied using the E158 beam at SLAC ($5 \times 10^{11} e^-$/pulse at 45-GeV, 200-300 ns pulse width, and focusable to small spots).

Positron yield is defined as the number of positrons captured in the predamping ring divided by the number of electrons incident on the target. The NLC has adopted the use of L-band (1.4 GHz) for both the initial 250-MeV capture and 1.75-GeV booster linacs. The larger aperture and longer wavelength of the L-band affords a factor of about 30 increase in acceptance over an S-band system. The design acceptance goal of the combined capture, booster, and predamping-ring systems has been set to 0.03 m-rad. Yield into this acceptance is calculated based on the initial e^+ distribution, generated using EGS4. In order to keep the peak shock stress in the target below the threshold for damage, three e^+ targets operating in parallel are required to produce the NLC beam. To assure overall system availability, a layout has been adopted where there are four target/capture modules, three of which are operating at any one time. Access is possible to the fourth target/capture module for maintenance and repair while the other 3 modules are in operation.

A schematic layout of the general features of the 3x4 NLC positron target system is shown in Fig. 5.3. Using an rf deflector, 6.2-GeV electron bunches, incident from the left-hand side of the figure, are separated into three trains . The three trains are directed onto three of the four e^+ target/capture modules. Each module contains a rotating, water-cooled target and flux concentrator [19] assembly, followed by a 250-MeV L-band linac for capture and initial acceleration. The three streams of 250-MeV positron bunches are combined into the standard NLC bunch format using another rf deflector section. The 250-MeV full bunch train is then accelerated to 1.98 GeV in an L-band linac, situated off the right-hand side of the figure. Shielding of the target vaults is required to permit access to the fourth target region while the other three are in operation. Several different layouts of the 3x4 positron scheme are being considered to optimize both operational efficacy and initial cost. They are all functionally identical. Table 5.4 lists the single target and capture section parameters.

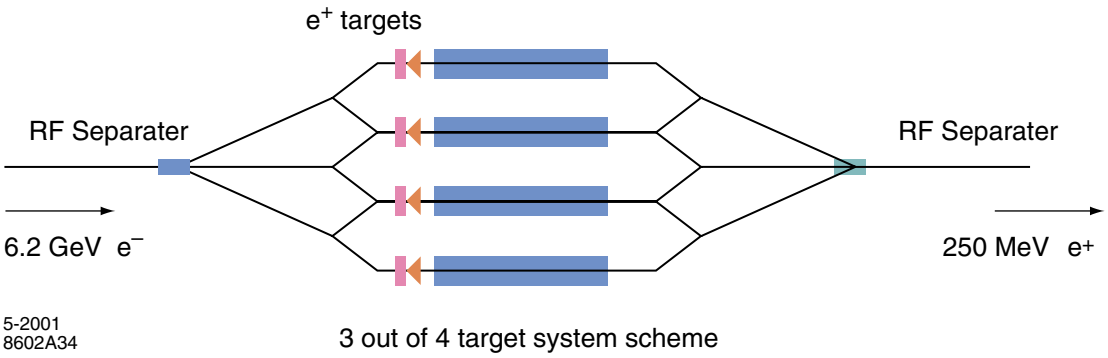

Figure 5.3: Schematic of the 3x4 NLC positron target system

Table 5.4: NLC Positron Source Parameters of the individual targets, 3 are operated in parallel, for case of 1.4 and 2.8 ns bunch spacing.

PARAMETER NAME	SYMBOL	VALUE	UNITS
Bunch Spacing	T_B	1.4 (2.8)	ns
TARGET			
Drive Beam Energy	E	6.2	GeV
Drive Beam Energy Spread	ΔE	1	% full width
Electrons/Bunch on Target	n_B	1.5 (3)	10^{10} particles
e^- Bunch-to-Bunch Pop. Uni.	$\Delta n_B/n_B$	<0.5	% rms
Number of Bunches	N_B	63 (32)	#
Incident Beam Radius	σ_r	1.6	mm rms
Repetition Rate	f	120	Hz
Drive	P_b	113	kW
Target Material		$W_{75}Re_{25}$	
Target Thickness	L_T	4	Rad. Length
Peak Energy Deposition	$\Delta E/\Delta vol$	35	J/g
Absorbed Target Power	P_T	16	kW
POSITRON CAPTURE			
RF Frequency	f_{rf}	1428	MHz
Bunch Length	ΔT	60	ps full width
Capture Energy	E_C	250	MeV
Capture Emittance (norm. edge)	$\gamma\varepsilon_{x,y}$	0.03	m-rad
Pre-DR Acceptance (norm.)	γA	0.045	m-rad
Yield@ 250 MeV	Y_C	1.4	e^+/e^-
Yield@ 1.98 GeV into γA = 0.03 m-rad	Y_{PDR}	0.6	e^+/e^-

A 6.2-GeV electron drive beam is used to create the positrons. This system is based on S-band technology. Because of the need to use three quasi-independent target/capture sections for positron production, the electrons will be generated using a photocathode-based source. Fine tuning of the individual electron bunch populations within the drive train is possible through bunch-to-bunch intensity adjustments

at the source laser. The unpolarized electron source system is essentially identical to the polarized electron source with the exception that shorter laser wavelengths and photocathodes with higher quantum yields will be used. The parameters of the electron drive beam are listed in Table 5.5.

Table 5.5: Drive Linac Electron Beam Parameters

PARAMETER NAME	SYMBOL	VALUE	UNITS
Bunch Spacing	T_b	1.4 (2.8)	ns
Energy	E	6.2	GeV
Bunch Energy Variation	$\delta E/E$	1	% Full Width
Single Bunch Energy Spread	$\sigma_{\Delta E/E}$	1	% Full Width
Emittance (norm. rms)	$\gamma\varepsilon_{x,y}$	100.0	10^{-6} m-rad
Bunch Length	σ_z	1.6	mm
Particles/Bunch	n_B	1.5 (3)	10^{10} particles
Train Population Uniformity	$\Delta n_T/n_T$	1	% Full Width
Bunch-to-Bunch Pop. Uniformity	$\Delta n_B/n_B$	2	% rms
Number of Bunches	N_b	190 (95)	#
Repetition Rate	f	120	Hz
Horizontal Beam Jitter	X/σ_x	10	%
Vertical Beam Jitter	Y/σ_y	10	%
Beam Power	P_b	340	kW

The present design is a conventional, reasonably well-understood methodology for producing positrons which can be expected to work if properly designed. As discussed in section 5.7, the production of polarized positrons is also being investigated. One outgrowth of these studies will be the development of an alternative unpolarized positron source based on a planar wiggler, similar to the TESLA design, but designed to meet the NLC performance requirements. The initial design will then be compared to the conventional design in regards to the usual metrics of cost, risk, and technical feasibility. A wiggler-based system should eliminate the need for multiple targets, may ease the requirements on the predamping ring, obviates the 6-GeV drive linac, and provides a straightforward upgrade path to polarized positrons. Of principal concern are the logistical issues associated with providing a high-energy electron beam (~150 GeV) and developing an injector commissioning strategy in which initial positron production must await significant progress in the operation of the electron injector and main linac. The installation and commissioning of the conventional positron source are independent of the schedule of the electron systems.

5.5 Damping Rings

The NLC damping rings are designed to damp the incoming electron and positron beams to the small emittances needed for collisions. The rings have three purposes: (1) damping the incoming emittances in all three planes; (2) damping incoming transients and providing a stable platform for the downstream portion of the accelerator; and (3), delaying the bunches so that feedforward systems can be used to compensate for charge fluctuations. To meet these goals, three damping rings have been designed: two identical main damping rings, one for the electrons and one for the positrons, and a predamping ring for the positrons [21,22]. The predamping ring is needed because the emittance of the incoming positrons is much larger than that of the electrons. Each damping ring will store multiple trains of bunches at once. At every machine cycle, a single fully damped bunch train is extracted from the ring while a new bunch train is injected. In this manner, each bunch train can be damped for many machine cycles.

The parameters of the two main damping rings are similar to the present generation of synchrotron light sources and the B-Factory colliders in that they must store high-current beams (~ 1 A) while attaining small normalized emittances. Table 5.6 compares the NLC ring parameters with those of the SLAC B-Factory Low-Energy Ring (PEP-II LER), the Advanced Light Source (ALS) at Lawrence Berkeley National Laboratory, and the Accelerator Test Facility (ATF) damping ring at KEK in Japan, which was built to verify many of the damping-ring design concepts. In particular, the stored beam currents are less than half of what the PEP-II LER has achieved, while the emittance, energy, and size of the rings are similar to those of the ALS and the ATF. These other rings have been largely successful in meeting their design parameters, and have been able to test and verify many of the accelerator physics and technology issues that will arise in the NLC damping rings.

Table 5.6: Comparison of NLC main damping rings with design parameters of other rings.

PARAMETER NAME	NLC MDR	PEP-II LER	LBNL ALS	KEK ATF
Energy (GeV)	1.98	3.1	1.5	1.54
Circumference (m)	300	2200	197	139
Current (A)	0.8	2.16	0.4	0.6
$\gamma\varepsilon_{x,\,equilib.}$ (10^{-6} m-rad)	2.17	400	12	4.3
$\gamma\varepsilon_{y,\,equilib.}$ (10^{-6} m-rad)	0.014	12	0.12	0.03

Strong coupled-bunch instabilities have been studied in the high-current B-factories, and have been successfully controlled using broadband, bunch-by-bunch feedback systems. Rapid damping of coupled-bunch motion has been demonstrated in the presence of these feedback systems at the ALS and B-factories, and damping rates in excess of 10^4 s^{-1} have been observed [23,24,25].

Issues associated with the very small beam emittances, such as intrabeam scattering and ion trapping, continue to be studied in the ALS and ATF [26,27]. A summary of measured parameters for the ATF is shown in Table 5.7, and work continues to improve the performance and diagnostics of that machine. The ATF has achieved a vertical emittance close to that desired in the main damping rings. Experiments have also been performed at low energy (1 GeV) in the ALS, where the measured emittances at 1 x 10^9 particles are $\gamma\varepsilon_x$ = 4 x 10^{-6} m-rad and $\gamma\varepsilon_y$ = 0.07 x 10^{-6} m-rad. These measurements, combined with theoretical modeling, are designed to improve the understanding of the process of intrabeam scattering in electron storage rings, and increase confidence in the predictions for the NLC damping rings.

Table 5.7: Achieved beam parameters at the ATF.

PARAMETER NAME	ACHIEVED
Energy (GeV)	1.28
Bunch population	1.2 x 10^{10}
$\gamma\varepsilon_x$ (10^{-6} m-rad)	3.5 ± 0.75
$\gamma\varepsilon_y$ (10^{-6} m-rad)	0.038 ± 0.006

In addition, the PEP-II LER at SLAC, the KEK-B LER at KEK, and the Advanced Photon Source (APS) at Argonne have studied the photoelectron-positron instability and have had success in controlling and understanding the phenomenon [28]. Simulations based on a simple circular vacuum chamber predict that the threshold for multipactoring occurs at several times the NLC bunch current, and growth times of transverse instabilities driven by the electron cloud are greater than 100 μs and can be controlled with a broadband feedback system. The NLC vacuum-system design includes an antechamber in which syn-

chrotron radiation is absorbed, significantly reducing the number of photoelectrons in the beam duct and further reducing the effects predicted for a simple circular cross section. At this stage it appears unnecessary to coat the aluminum vacuum chambers with low secondary-emission yield materials such as TiN.

The similarities with other rings have also simplified the design process for NLC, and experience at these other accelerators will continue to be applied to benefit the damping-ring designs. For example, the damping ring rf system is based on the higher-order-mode damped cavity designs successfully operating at the SLAC B-Factory and the ATF damping ring; the multibunch feedback systems are based upon the feedback systems successfully verified at the SLAC B-Factory and the ALS, and the vacuum system is similar to that used by the ALS [24,29,30]. Furthermore, the design uses 'C' quadrupole and sextupole magnets similar to those used at the ALS and the APS, a high-field permanent-magnet wiggler similar to those in use at third-generation light sources, and a double kicker system for extraction similar to one operational in the ATF. The successful demonstration of these and other systems and components allows a high degree of confidence in achieving the NLC damping-ring parameters.

The NLC damping-ring complex is designed to operate with the parameters listed in Table 5.8. These design parameters exceed the requirements of all presently considered NLC upgrades. The rings produce extracted electron and positron beams with emittances $\gamma\varepsilon_x = 3\text{x}10^{-6}$ m-rad and $\gamma\varepsilon_y = 2\text{x}10^{-8}$ m-rad, at a repetition rate of 120 Hz. Designs have also been developed which allow repetition rates as high as 180 Hz, however in this case the use of two main damping rings per complex is proposed [31]. The beams in the damping rings consist of multiple trains of 190 bunches with an injected single bunch charge of $0.8\text{x}10^{10}$. To provide operational flexibility, the rings have been designed also to accommodate trains of 95 bunches spaced by 2.8 ns with maximum single bunch charge of $1.6\text{x}10^{10}$ in the main rings ($1.8 \text{ x } 10^{10}$ in the predamping ring), and to operate with a peak current roughly 15% higher than the nominal peak current. In addition, the rings have been designed to operate at 1.98-GeV, with an energy range of ±5 %. This will allow the damping rate to be adjusted if necessary.

Table 5.8: Requirements for NLC Main Damping Rings.

PARAMETER NAME	VALUE
$\gamma\varepsilon_{x\ equilib.}/\gamma\varepsilon_{x\ extract.}$ (10^{-6} m-rad)	3.0 / 3.0
$\gamma\varepsilon_{y\ equilib.}/\gamma\varepsilon_{y\ extract.}$ (10^{-6} m-rad)	0.014 / 0.020
Bunches per train	190 / 95
Bunch spacing (ns)	1.4 / 2.8
Bunch population	$0.8 \text{ x } 10^{10}$ / $1.6 \text{ x } 10^{10}$
Repetition rate (Hz)	120

At present, most of the studies have concentrated on the main damping rings. Engineering studies have been performed for key systems such as vacuum, damping wigglers, and rf systems, and a good outline of the design and the expected problems has been developed [21]. In particular, the most difficult issues have been identified and solutions described: these are the dynamic aperture, the vertical emittance, the impedance and instabilities, and the stability and jitter in both longitudinal and transverse phase space. As stated, much of the design rests on work performed for operational facilities including the B-factories and the ATF. In most aspects, the predamping ring has relatively loose requirements. The emittance, damping time and beam stability requirements are not severe. The two main challenges are the large dynamic aperture needed and the injection/extraction kicker systems. The design is still in a preliminary stage but these challenges have been addressed.

5.5.1 Main Damping Rings

The NLC main damping rings are roughly 300 m in circumference and measure 60 m by 100 m with a nominal energy of 1.98-GeV. The rings are designed in a racetrack form with two arcs separated by straight sections; the layout is illustrated in Fig. 5.4 [32]. The main damping rings are designed to damp beams with injected emittances $\gamma\varepsilon_{x,y} = 1.5\text{x}10^{-4}$ m-rad to extracted beam emittances of $\gamma\varepsilon_x = 3\text{x}10^{-6}$ m-rad and $\gamma\varepsilon_y = 2\text{x}10^{-8}$ m-rad. The rings will operate at 120 Hz. They provide sufficient damping to decrease the injected emittance by four orders of magnitude. These parameters are summarized in Table 5.9 for the main damping rings (MDR), and the positron predamping ring (PPDR). The main damping- ring lattice is based on detuned Theoretical Minimum Emittance (TME) cells utilizing combined-function bending magnets. This lattice type was chosen because of efficiency in generating low emittance and eased requirements on the combined-function bending magnets. The chromaticity is corrected with two families of sextupoles and the dynamic aperture is more than sufficient. The damping is performed using both high-field bending magnets and ten 4.6-meter sections of damping wiggler.

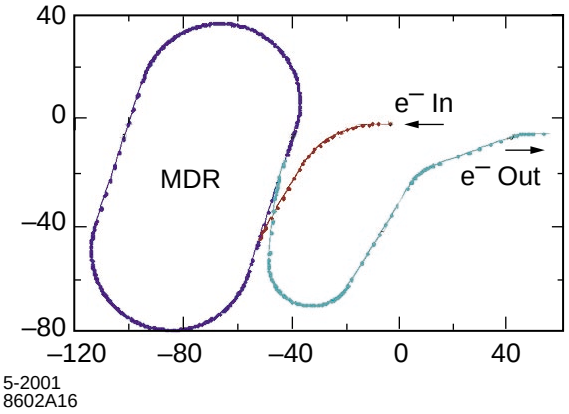

Figure 5.4: Layout of main damping ring.

The dynamic aperture is predicted to be in excess of 15 $\sigma_{injected}$, including effects of errors [32]. Figure 5.5 shows beam survival tracked over 500 turns, including in (b) systematic errors in dipoles, quadrupoles, and sextupoles. Potential limitations due to the contribution from the 46 meters of wiggler magnet have been studied. Analytical expressions of arbitrary three-dimensional wiggler fields have been developed, and tracking including the nonlinear components of the wiggler field will be used to determine the minimum pole width requirement for the 2.15 T hybrid wiggler magnet [33]. Preliminary analysis indicates that the wiggler with a magnet pole width of 11 cm does not seriously degrade the dynamic aperture.

The rings operate with three trains of 190 bunches. The bunch trains are injected onto and extracted from the closed orbit using pulsed kickers and DC septa. To avoid coupled-bunch instabilities, the rf cavities are higher-order-mode damped based on those of the PEP-II B-Factory and a transverse bunch-by-bunch feedback system is used. As stated, the rings are designed to operate with maximum bunch charges of $1.6\text{x}10^{10}$ particles; this is roughly 10% more than the maximum needed at the IP. In addition, the electron source has been designed to provide additional charge to allow for at least 10% losses during injection into the electron damping ring. Similarly, the positron source has been designed to produce at least 20% additional charge to provide for losses during injection into the predamping ring [34].

Table 5.9: Parameters for Main Damping Rings and the Predamping Ring.

PARAMETER NAME	MDR	PPDR
Circumference (m)	299.792	218.336
Energy (GeV)	1.98	1.98
Max. Current (A)	0.8	0.75
Max. Rep. Rate (Hz)	120	120
Bunch trains x Bunches per train	3 x 190	2 x 190
Train / Bunch separation (ns)	65 / 1.4	65 / 1.4
ν_x, ν_y, ν_s	27.26, 11.14, 0.0035	8.91, 7.24, 0.031
$\gamma\varepsilon_{x\ equilib.}$ (m-rad)	2.17×10^{-6}	103×10^{-6}
$\gamma\varepsilon_{x\ extract.}$, $\gamma\varepsilon_{y\ extract.}$ (m-rad)	2.18×10^{-6}, 0.02×10^{-6}	114×10^{-6}, 69×10^{-6}
$\sigma_{\Delta E/E}$, σ_z	0.09 %, 3.6 mm	0.09 %, 7.2 mm
$\zeta_{x\ uncorr.}$, $\zeta_{y\ uncorr}$	-37.12, -28.24	-10.39, -12.23
τ_x, τ_y, τ_ε (ms)	4.85, 5.09, 2.61	4.24, 5.13, 2.87
U_{sr} (kV/turn)	777	561
α_p	2.95×10^{-4}	7.05×10^{-3}
V_{RF}, Frequency	1.07 MV, 714 MHz	3.4 MV, 714 MHz
Lattice	36 TME cells	16 TME cells

Finally, because the rings must generate extremely small beam emittances, there are tight jitter and alignment tolerances. Extensive effort has been made to include cancellations and tuning procedures in the design that will ease the tolerances to reasonable levels. Skew quadrupole windings will be incorporated in sextupole magnets to facilitate coupling correction. Quadrupoles and sextupoles will have independent trim control, and magnet movers will be used to facilitate beam-based alignment .

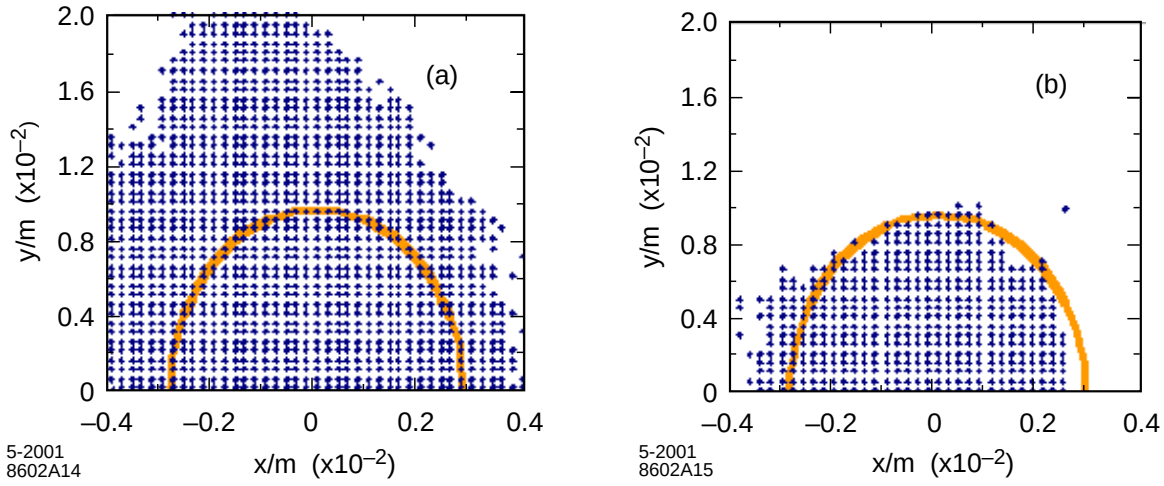

Figure 5.5: Dynamic aperture plots a) without errors, b) with combined systematic errors in dipoles, quadrupoles, and sextupoles. The half ellipse shows 15 times the injected beam size.

5.5.2 Positron Predamping Ring

The predamping ring has a racetrack form with dispersion-free straight sections for injection and extraction, and damping wigglers of total length roughly 25 m. The ring is roughly 60 meters by 40 meters and is illustrated schematically in Fig. 5.6. In the design, the injection and extraction regions are in the straight sections on opposite sides of the ring. To reduce the requirements on these components, the systems are designed to occupy most of these regions. To minimize rf transients during injection and extraction, a new bunch train will be injected one half turn after a train is extracted. In addition, the rf cavities are placed downstream of the injection kicker and upstream of the extraction kicker so that the injection/extraction process will not interrupt the beam current seen by the cavities.

The positron predamping ring is designed to damp the large emittance beam from the positron source to an emittance of roughly $\gamma\varepsilon_{x,y} = 1.5\text{x}10^{-4}$ m-rad; these parameters are summarized in Table 5.9. The extracted positrons are then injected into the main damping ring where they are damped to the desired final emittances. The predamping ring allows the large aperture requirements for the incoming positron beams to be decoupled from the final emittance requirements of the linear collider. The predamping ring does not need to produce flat beams, so to maximize the damping of the transverse phase space, the ring may operate on the coupling difference resonance. This increases the damping in both the horizontal and vertical planes. Like the main damping ring, the ring damps multiple trains of bunches at once.

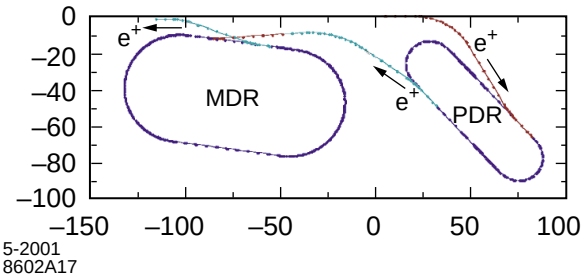

Figure 5.6: Layout of the positron damping ring and predamping ring.

The magnets and vacuum systems are designed to provide sufficient aperture to accept a 2-GeV beam with an edge emittance of $\gamma\varepsilon_{x,y} = 0.03$ m-rad and momentum spread of $|\delta p/p| = 1.5\%$ plus betatron-action jitter of $\Delta\gamma\varepsilon_{x,y} = 0.015$ m-rad for misalignments and missteering. Given the nominal injected edge emittance of $\gamma\varepsilon_{x,y} = 0.03$ m-rad, this provides a substantial margin for injection and internal mismatches. In addition, the injector specifications allow significant overhead for injection losses into the predamping ring [34]. The predamping ring is designed to operate with a maximum bunch charge that is roughly 10% greater than the maximum required at the IP. Like the main damping rings, quadrupoles and sextupoles will have independent trim control, and magnet movers will be used to facilitate beam-based alignment as well as matching of the lattice functions, which is especially important in the predamping ring because of the limited aperture.

5.5.3 Outstanding issues

Measurements of intrabeam scattering and minimum achievable emittance within the parameter range of the NLC damping rings will continue at the ATF, ALS and other machines. These measurements, combined with theoretical modeling, will improve our understanding of the process of intrabeam scattering, and confidence in predictions for the damping rings. Modifying the electron cloud simulations to include an antechamber will allow an improved estimate of the effect in the positron rings, and ion effects in the electron ring will be studied. Tracking studies using realistic wiggler fields will allow better definition of the pole width requirements to maintain sufficient dynamic aperture in the machine.

A residual vacuum pressure of 10^{-9} torr is required to alleviate ion effects. In the arcs, adequate pumping is expected from large ion pumps located directly under discrete photon stops in the antechamber. In the wiggler vacuum chamber, however, distributed pumping may be required to accommodate thermal outgassing in the vacuum chamber which has a large surface area and low conductance at the beam duct. While a design for such a distributed pumping scheme has been developed, improved methods of vacuum chamber fabrication are also being investigated to reduce the surface outgassing rate and avoid the necessity of distributed pumping. Various machining and cleaning techniques are under investigation, and accurate outgassing measurements of samples are being made using apparatus capable of measuring 10^{-12} torr l s^{-1} cm^{-2}.

5.6 Bunch Length Compressors

The NLC bunch compressors [35] must reduce the ~4 mm rms length of the bunches extracted from the damping rings to the 90-140 μm bunch length required for the main linacs and final-focus systems. A two-stage compressor system has been designed where the first stage follows the damping ring and the second stage is at the exit of the S-band prelinac at a beam energy of 8-GeV. Electron and positron bunch-compression systems are identical. The bunch-compressor system has been designed to meet the following additional goals: (1) Expected multibunch phase variations in the damping ring of up to ±5 mm should not produce relative energy variations that are much larger than ±0.1 % in the final-focus systems. (2) The system should include a 180° turn-around arc to permit future main-linac extensions and to allow beam abort and feedforward systems. (3) The transverse emittances must be preserved to within a reasonable budget with diagnostics and correction elements included in the design. (4) The compression systems should not depolarize the beams.

The two-stage system has a number of advantages over a single-stage compressor. In particular, it keeps the rms energy spread less than about 2%; it is optically more straightforward; and the bunch length is more naturally matched to the acceleration rf frequency so that energy spread due to the longitudinal wakefields can be cancelled locally. The disadvantage of the two-stage design is that it is more complex and lengthy than a single-stage compressor. The first stage rotates the longitudinal phase by $\pi/2$ while the second stage performs a 2π rotation. In this manner, phase errors due to the beam loading in the damping rings and energy errors due to imperfect multibunch energy compensation in the 6-GeV S-band prelinacs do not affect the beam phase at injection into the main linac.

Assuming an rms energy spread of $\sigma_{\Delta E/E} = 1 \times 10^{-3}$ and rms bunch length of $\sigma_z = 5$ mm, the first stage compresses the damping ring beam to a bunch length of about 500 μm. This stage consists of a 140-MeV L-band (1.4-GHz) rf section followed by a long-period wiggler which generates the momentum compaction, R_{56}, needed for the bunch compression. The second bunch-compression stage follows the prelinac. Assuming an rms bunch length of $\sigma_z = 500$ μm, it compresses the beam to a bunch length of 90 μm. This compressor is a telescope in longitudinal phase space which rotates the phase space by 2π. It consists of a 180° arc which is followed by a 600-MeV X-band (11.4-GHz) rf section and a chicane. Adjustments to the low energy compressor rf voltage and wiggler strength permit control of the final bunch length over the specified range of 90-140 μm for fixed settings of the high energy compressor. Figure 5.7 illustrates the layout of the NLC bunch compression system. Beam parameters are listed in Table 5.10.

One of the driving philosophies behind the NLC compressor design has been to utilize naturally achromatic magnetic lattices wherever the beam energy spread is large. In particular, the optics is chosen so that quadrupoles are not placed in regions of large dispersion and strong sextupoles are not needed. This choice arises from experience with the SLC bunch compressors [36] which were based on second-order achromats in which quadrupoles are located in dispersive regions and strong sextupoles are used to cancel the chromatic aberrations. Unfortunately, the SLC design was difficult to operate and tune because of large nonlinearities and sensitivity to multipole errors in the quadrupoles; over the years, additional nonlin-

ear elements were added (skew sextupoles and octupoles) to help cancel the residual aberrations but tuning remained problematic. To facilitate tuning, orthogonal tuning controls and diagnostics have been explicitly designed into the NLC system, making the system relatively straightforward to operate.

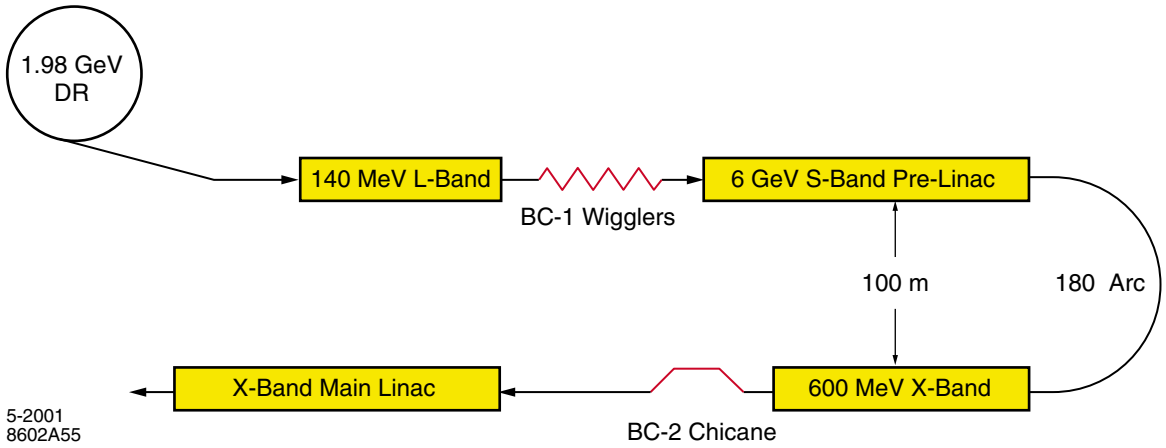

Figure 5.7: The NLC two-stage bunch length compression system. The first stage of compression consists of an L-band rf section followed by a dipole wiggler, operating and 1.98- GeV. The second stage of compression includes the 6-GeV prelinac, 180° turn-around arc, a 600-MeV X-band rf section and a dipole chicane. Beam diagnostics are included to permit full tune-up and control.

As discussed, the rf acceleration in the first-stage compressor system is performed with relatively low frequency L-band rf (1.4 GHz). Although this system is, in general, more expensive than higher frequency rf, it has a larger acceptance which is needed at the lower beam energy. In particular, the system has been designed to have small beam loading and relatively loose alignment tolerances. This is important to provide the desired reliability and stability. Finally, although the tolerances on components in the bunch compressor systems are not nearly as tight as in the main linacs or the final-focus systems, the same methods of beam-based alignment and tuning have been adopted. In particular, to ease the alignment procedures, all of the quadrupoles will be mounted on magnet movers. In addition, each quadrupole will contain a BPM with a resolution of 1 μm. Similarly, all of the accelerator structures will be instrumented with rf BPMs to measure the induced dipole modes and each girder will be remotely movable for minimization of wakefields.

Table 5.10: Input and Output Beam Parameters of the BC-1 and BC-2 Systems.

PARAMETER NAME	SYMBOL	INPUT	VALUE	UNIT
BUNCH COMPRESSOR 1				
Energy	E	1.98	1.98	GeV
Single Bunch Energy Spread	$\sigma_{\Delta E/E}$	0.2	2	% Full Width
Bunch Length	σ_z	5	0.5	mm, rms
BUNCH COMPRESSOR 2				
Energy	E	8	8	GeV
Single Bunch Energy Spread	$\sigma_{\Delta E/E}$	0.5	3.2	% Full Width
Bunch Length	σ_z	500	90-150	μm, rms

As noted in section 5.2, there are presently two layout scenarios under consideration for the NLC injector systems. Concerning the issue of bunch length compression, it should be noted that a centralized injector requires more bending through the beam turn-arounds than a remote injector. Since arc momentum compaction and synchrotron radiation emittance dilution depend on the absolute value of the net bend angle, the arc cell design has a different optimal configuration [35]. A methodology has been developed to minimize overall system costs while meeting the design goals. Designs for both layouts meet the NLC bunch-compression requirements.

5.7 Polarized Positrons

The only practical way to produce polarized positrons for a linear collider is through pair creation using circularly polarized photons. In principle, positrons can be polarized in a storage ring but the rate of polarization build-up is relatively low, making the storage time required prohibitively long. For pair creation, the required energy of the photons falls in the range of 10-60 MeV. There are three candidate methods for producing circularly polarized photons, generation through bremsstrahlung from polarized electrons [37], production from Compton backscattering of polarized laser photons off an unpolarized electron beam [38], and emission of polarized photons from a high-energy electron beam in a helical undulator [39]. The first method has low estimated conversion efficiencies and is not a primary candidate. The remaining two methods, Compton based and undulator based, both have significant technical issues to be resolved.

For Compton generation of polarized photons, extremely intense laser beams are required. On the other hand, the requirements on the electron beams are relatively modest; the energy of the electrons is in the range of several GeV. Furthermore, the helicity of the positrons is easily flipped on a pulse-to-pulse basis by switching the sign of the incident laser photon polarization. This ability to randomly and rapidly change the positron helicity is of significant interest to the experimenters. For undulator-based photon generation, present designs require high-energy, low-emittance electrons. The emittance requirements prevent the utilization of the post-collision, disrupted electron beam. The energy of the electron drive beam is 150 GeV or above for undulator periods in the range of a centimeter. Use of the undulator precludes rapid changes in the helicity of the positrons. The JLC has developed a design for polarized positrons based on Compton production [40]. TESLA has developed a design which uses an undulator [20]. Requirements for the photon conversion to polarized positrons and subsequent selective collection of the most energetic positrons for maximum polarization are essentially the same in both designs.

NLC is presently studying both options, which would ultimately lead to a design similar to one of the existing design proposals. The present plan for the NLC efforts are to reproduce the existing JLC and TESLA design studies as a means of developing the necessary tools and expertise. This effort is initially concentrated on understanding the conversion and collection of positrons. This will result in a projection of photon-to-polarized- positron yield captured by a predamping ring. The yield calculation allows the specification of the required number of incident photons, which drives the requirements on the methods of photon production. Figure 5.8 shows a possible layout for an NLC polarized positron system which is based on a helical undulator. In Fig. 5.8, a dedicated electron beam for photon production is produced through doubling the repetition rate of the first part of the electron main linac and sending it through an undulator. Possible alternatives include using the colliding electron beam which could be extracted from the main linac at an energy of about 150 GeV, passed through an undulator and reinjected into the main linac for further acceleration and transport to the IP.

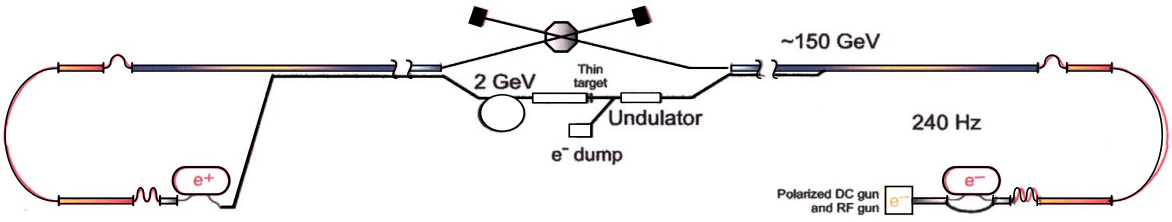

Figure 5.8: An undulator-based source of polarized positrons using a separate high energy electron beam.

5.8 Present Activities and Future Plans

The thrust of the present R&D and design activities fall into three broad categories: (1) improving the technical foundation of the NLC injector systems design through feasibility demonstrations, technology reviews, and augmented system simulations; (2) developing alternate schemes to assure the realizability of the designs; and (3), investigating the feasibility of novel options which improve either the operability or capability of the overall design. As discussed above, it is a goal of the R&D effort to demonstrate the full NLC polarized electron charge and current density. It is important to determine the maximum, survivable energy deposition in an NLC positron target. Demonstration of the NLC damped beam emittances and improved experimental understanding of damping-ring collective effects are priorities.

The present design of the positron generation system is based on limiting the peak energy deposition and integrated fluences in the targets to the level of the SLC positron target. Ongoing research is aimed at developing better target material and at improving the understanding of fatigue and radiation damage in a positron target. Although not presently included in the injector design, considerable thought and effort are going into the studies on the feasibility and efficacy of polarized rf guns and sources of polarized positrons. Because of the considerable work to be done in the development of both of these systems, neither are presently included as part of the present design configuration. The current design does not preclude the future adoption of either or both systems into the NLC complex at a later time.

Many of the requirements and systems needed to achieve the NLC damping-ring parameters have been demonstrated in other rings, such as the B-factories, the ALS, and the ATF. Additional experiments and theoretical studies are planned to further understand and predict behavior in the damping rings and through the extraction system. Investigations are focused on intrabeam scattering, electron cloud and ion driven instabilities, dynamic aperture limitations, extraction system stability, and vacuum systems technologies.

References

[1] Alley, R., et al., "The Stanford Linear Accelerator Polarized Electron Source," *Nucl. Instr. and Meth*., **A365**:1-27, 1995 (also SLAC-PUB-6489, March 1995).

[2] Krejcik, P., et al., 'Recent Improvements in the SLC Positron System Performance," *Proc. 3rd EPAC*, Berlin, 1992 (also SLAC-PUB-5786, March 1992).

[3] Bane, K. and Li, Z., "Dipole Detuning in the Injector Linacs of the NLC," LCC-0043, July 2000.

[4] Allen M.A., et al., "Performance of the SLAC Linear Collider Klystrons," Proc. PAC 1987, Washington, D.C., 1987 (also SLAC-PUB-4262, March 1987).

[5] Nakanishi, T., et al., "Highly Polarized Electron Source Development in Japan," *1st APAC 1998*, Tsukuba, Japan, March 1998.

[6] Mulhollan, G.A., et al*.,* "Photovoltage Effects in Photoemission from Thin GaAS Layers," *Phys. Lett*. **A282**:309-318, 2001 (also SLAC-PUB-8753, Mar 2001).

[7] Togawa, T., et al., "Production of Polarized Electron Beam with Sub-nanosecond Multibunch Structure from Superlattice Photocathode," *Nucl. Instr. and Meth.* **A455** 118, 2000.

[8] PPRC Private Communication, May 2001.

[9] Matsumoto, H., et al., "High Power Test of a SLED System with Dual Side Wall Coupling Irises for Linear Colliders," *Nucl. Instr. and Meth*. **A330** 1, 1993 (also KEK-PREPRINT-92-179, January 1993).

[10] Blockus, D., et al., "Proposal for Polarization at the SLC," SLAC-PROPOSAL-SLC-UPGRADE-01 (1986).

[11] Emma, P., "A Spin Rotator System for the NLC," NLC-Note-7, December 1994.

[12] Aleksandrov, A.V., et al., "Experimental Study of GaAs Photocathode Performance in RF Gun," *Proc. PAC 1999*, New York, N.Y. 1999.

[13] Aulenbacher, K., et al., "RF Guns and the Production of Polarized Electrons," CERN-CLIC-NOTE-303, SLAC-NLC-NOTE-20, May 1996.

[14] Krejcik, P., et al., 'Recent Improvements in the SLC Positron System Performance," *Proc. 3rd EPAC*, Berlin, 1992 (also SLAC-PUB-5786, March 1992).

[15] Maloy, S., et al., "SLC Target Analysis," LANL LA-UR-01-1913, June 2001.

[16] Stein, W., *"*Thermal Shock Structural Analyses of the SLC Positron Target,*"* Lawrence Livermore National Laboratory, Livermore, California, UCRL-PRES-142893, April 24, 2001.

[17] Caturla, M., Private Communication, May 2001.

[18] Sunwoo, A., et al., "Characterization of Virgin W-Re Material," Lawrence Livermore National Laboratory, UCRL-PRES143841, April 24, 2001.

[19] Kulikov, A.V., et al., "SLC Positron Source Pulsed Flux Concentrator," *Proc. PAC 1991*, San Francisco, CA, 1991 (also SLAC-PUB-5473 June 1991).

[20] Bialowons, W., et al., "Conceptual Design of a 500 GeV e+e- Linear Collider with Integrated X-ray Laser Facility (Tesla Design Report)," DESY 1997-048, May 1997, 416 ff.

[21] Corlett, J.N., et al., "The Next Linear Collider Damping Ring Complex," *Proc. PAC 2001*, Chicago, 2001.

[22] Wolski, A. and Corlett, J.N., "The Next Linear Collider Damping Ring Lattices," *Proc. PAC 2001*, Chicago, 2001.

[23] Fox, J., et al., "Multi-bunch Instability Diagnostics via Digital Feedback Systems at PEP-II, DAFNE, ALS, and SPEAR," *Proc. PAC 1999*, New York, 1999.

[24] Barry, W., et al., "Operational Experience with the PEP-II Transverse Coupled-Bunch Feedback Systems," *Proc. PAC 1999*, New York, 1999.

[25] Byrd, J.M. and Barry, W., "Controlling the Vertical Mode Coupling Instability with Feedback in the Advanced Light Source," *Proc. PAC 1997*, Vancouver, 1997.

[26] Urakawa, J., et al., "Experimental Results and Technical Research and Development at ATF (KEK)," *Proc. EPAC 2000*, Vienna, Austria, 2000.

[27] Corlett, J.N., et al., "Measurements of Intra-Beam Scattering at Low Emittance in the Advanced Light Source," *Proc. HEACC 2001*, Tsukuba, Japan, 2001.

[28] Furman, M., et al., "Electron-Cloud Measurements and Simulations for the APS," *Proc. PAC 2001*, Chicago, 2001.

[29] Rimmer, R.A., et al., "RF cavity R&D at LBNL for the NLC Damping Rings, FY1999," CBP Tech Note 196, LCC-0033, LBNL, Berkeley, November 1999.

[30] "1-2 GeV Synchrotron Radiation Source," PUB-5172, LBNL, Berkeley, 1986.

[31] Wolski, A., "Improved Dynamics in the 180 Hz NLC Damping Rings," CBP Tech Note 223, LCC-0055, LBNL, Berkeley, 2001.

[32] Wolski, A., "Lattice Description for NLC Main Damping Rings at 120 Hz," CBP Tech Note 227, LCC-0061, LBNL, Berkeley, 2001.

[33] Wolski, A., "Symplectic Integrators for Nonlinear Wiggler Fields," CBP Tech Note 228, LCC-0062, LBNL, Berkeley, 2001.

[34] Sheppard, J.C., et al., "Update on the NLC Injector System Design," *Proc. PAC 2001*, Chicago, 2001.

[35] Emma, P., "Cost and Performance Optimization of the NLC Bunch Compressor Systems," LCC-0021, August 1999.

[36] Adolphsen, C. et al., "Chromatic Correction in the SLC Bunch Compressors," *Proc. PAC 1991*, 503-505, May 1991 (also SLAC-PUB-5584, June 1991).

[37] Potylitsin, A.P., "Production of Polarized Positrons through Interaction of Longitudinally Polarized Electrons with Thin Targets," *Nucl. Inst. and Meth*. **A398,** 395, 1997.

[38] Hirose, T., et al., "Generation of Polarized Positrons via Laser-Compton Scattering at the KEK Damping Ring," *1st APAC 1998*, Tsukuba, Japan, March 1998.

[39] Mikhailichenko, A.A., "Use of Undulators at High Energy to Produce Polarized Positrons, *Proc. Workshop on New Kinds of Positron Sources for Linear Colliders*, SLAC Report 502, 1997.

[40] Hirose, T., et al., "Polarized Positron Source for a Linear Collider, JLC," *Nucl. Instr. and Meth*. **A455**, 2000.